

# X Inactivation of the *OCNC1* Channel Gene Reveals a Role for Activity-Dependent Competition in the Olfactory System

Haiqing Zhao and Randall R. Reed\*  
Howard Hughes Medical Institute  
Department of Molecular Biology and Genetics  
Johns Hopkins School of Medicine  
725 N. Wolfe Street  
Baltimore, Maryland 21205

## Summary

The organization of neuronal systems is often dependent on activity and competition between cells. In olfaction, the X-linked *OCNC1* channel subunit is subject to random inactivation and is essential for odorant-evoked activity. Reporter-tagged *OCNC1* mutant mice permit the visualization of *OCNC1*-deficient olfactory neurons and their projections. In heterozygous females, X inactivation creates a mosaic with two populations of genetically distinct neurons. *OCNC1*-deficient neurons are slowly and specifically depleted from the olfactory epithelium and display unusual patterns of projection to the olfactory bulb. Remarkably, this depletion is dependent on odorant exposure and is reversed by odorant deprivation. This suggests that odorants and the activity they evoke are critical for neuronal survival in a competitive environment and implicate evoked activity in the organization and maintenance of the olfactory system.

## Introduction

In vertebrates, odor molecules activate receptors and a well-characterized signal transduction cascade in the olfactory neurons located in epithelial surface of the nasal cavity. Odorant-evoked action potentials propagate down the axons of these sensory neurons to the olfactory bulb where the signals are relayed to mitral and tufted cells that project to higher olfactory centers (Farbman, 1992; Shepherd, 1994). Each glomerulus in the olfactory bulb represents a site where critical synaptic connections are formed between primary olfactory cells expressing a particular odorant receptor and second order neurons. The olfactory system is precisely organized and highly dynamic. Each olfactory neuron achieves receptive specificity by expressing only one of about 1000 odorant receptor genes (Chess et al., 1994; Malnic et al., 1999). Additionally, olfactory neurons expressing the same odorant receptor, which are randomly dispersed in one of the four zones of the olfactory epithelium, converge axons into a small number of topographically fixed glomeruli within the bulb (Ressler et al., 1994; Vassar et al., 1994; Mombaerts et al., 1996). Olfactory neurons are replaced continuously throughout life (Graziadei and Graziadei, 1979; Mackay-Sim and Kittel, 1991), but the neuronal population maintains a conserved connection pattern to the olfactory bulb.

The influence of odorant-evoked activity on the olfactory system has been investigated by surgical and genetic manipulation. Using naris occlusion to block environmental odorant stimulation postnatally, major changes were observed in the olfactory bulb (Brunjes, 1994), including reductions in granule cell number (Frazier and Brunjes, 1988) and in tyrosine hydroxylase levels of periglomerular cells (Baker, 1990). The treatment also led to a thinner olfactory epithelium and a decrease in neuronal turnover in the epithelium (Farbman et al., 1988; Cummings and Brunjes, 1994).

A genetic disruption of the *OCNC1* gene, which encodes an essential subunit of the olfactory cyclic nucleotide-gated channel (OCNC) that is a key component in the olfactory signal transduction pathway, blocked all odorant-evoked activity in embryonic and neonatal mice (Brunet et al., 1996; Lin et al., 2000). These mice also possessed a thinner epithelium, reduced tyrosine hydroxylase levels, and downregulation of the activity-dependent marker, c-Fos, in the bulb (Baker et al., 1999). The pruning of mitral cell dendrites in mutant animals was modestly slowed but ultimately unperturbed (Lin et al., 2000). Additionally, the pattern of convergence was unaltered for olfactory neurons expressing several odorant receptors (Lin et al., 2000; Zheng et al., 2000), but the absence of *OCNC1* subtly perturbed targeting of M72 receptor-expressing neurons (Zheng et al., 2000). In each of these activity-deprivation paradigms, olfactory neurons were generated and projected axons into the bulb and the morphology of the olfactory epithelium as well as the olfactory bulb were grossly normal during development and the subsequent adult neuronal replenishment.

Neuronal activity contributes to organization of the nervous system through axonal remodeling and regulation of cell survival. These two processes are distinguished by the eventual fate of the projecting neuron. In the visual system, the remodeling of cortical projections are driven by activity-dependent competition (Katz and Shatz, 1996). Based on the classic paradigm of Hubel and Wiesel, anatomical studies highlighted the importance of competition by comparison of the innervation pattern in the visual cortex upon monocular and binocular deprivation (LeVay et al., 1980). Smaller cortical fields corresponded to the deprived eye while the projection fields from the stimulus-exposed retina were expanded. Interestingly, binocular deprivation led to somewhat normal innervation from both eyes. In other aspects of visual system development, organization and the pattern of connections arise through selective cell survival. Early in development, ganglion cells project both ipsilaterally and contralaterally to the superior colliculus. Those cells projecting to the ipsilateral side are preferentially lost. Activity-dependent competition appears to control this cell death since tetrodotoxin injection into the opposite eye leads to the survival of the ipsilateral projecting ganglion cells. When both eyes were treated with tetrodotoxin, no loss of the ipsilateral projecting neurons was seen on either side (Fawcett et al., 1984). In these two systems, remodeling or selective

\*To whom correspondence should be addressed (e-mail: rreed@jhmi.edu).

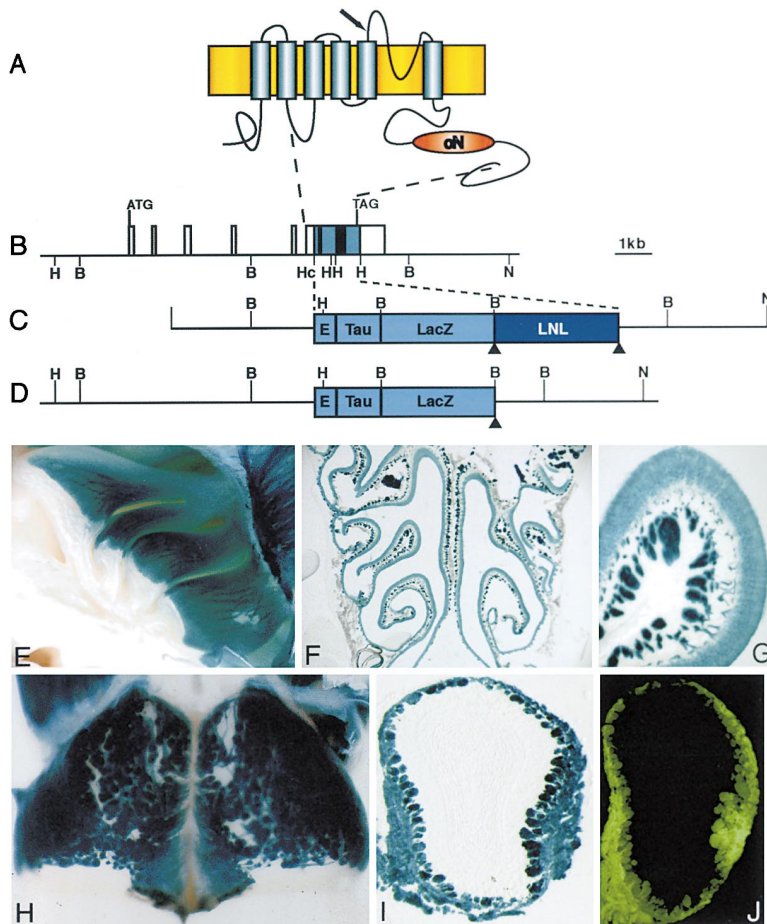


**Figure 1. Generation and Characterization of Reporter-Tagged OCNC1-Deficient Mice**

(A) Schematic of OCNC1 protein structure. Arrow indicates truncation site in OCNC1 disruption; cN, cyclic nucleotide binding domain. (B) OCNC1 gene structure. The exons are represented as open rectangles. The translation start site, stop site, and relevant restriction sites are indicated; H, HindIII; B, BamHI; Hc, HincII; N, NotI.

(C) Targeting vector. E, IRES, internal ribosomal entry site; tau, tau microtubule-associated protein; lacZ, encoding the  $\beta$ -galactosidase reporter; LNL, loxP-neo-loxP; solid triangle, loxP site.

(D) Structure of modified OCNC1 locus. Homologous recombination between targeting vector and the chromosomal DNA replaces a fragment (gray bar in [B]), containing the coding sequence for the conceptual pore domain and the cyclic nucleotide binding domain (black bars in [B]), with an IRES-tau::lacZ fragment or an IRES-tau::EGFP fragment (not shown) followed by an LNL cassette. The neo-selection marker was deleted by mating chimeric founder males with cre-transgenic female mice.

(E–J) Reporter expression in tagged OCNC1<sup>-/-</sup> hemizygous male mice reveals a structurally normal olfactory epithelium and bulb. Olfactory epithelium and bulb of tau::lacZ-tagged mice was stained with x-gal. (E) A whole mount view of the medial surface of nasal turbinates. Anterior is on the left. (F and G) Staining of coronal section of olfactory epithelium with x-gal at low (F) and high (G) magnification. Blue staining was restricted to olfactory neurons and the axon bundles residing beneath the epithelium. All neurons

appear to express the reporter. (H) A dorsal view of stained olfactory bulb in whole mount. Anterior is up. (I) A coronal section of an olfactory bulb. X-gal staining is present throughout the olfactory nerve layer and in all glomeruli. Dorsal is up, medial is on the left. (J) A coronal section of olfactory bulb from a tau::GFP-tagged mouse visualized by intrinsic fluorescence.

cell survival occur at defined periods of development. It is obviously interesting to determine the contribution of activity-mediated competition in a system where neuronal populations are continually turning over. The ability to control sensory input and evoked activity in olfactory neurons that are continually being replaced and projecting to a highly organized olfactory bulb represents an attractive system to examine the contributions of activity to neuronal organization and survival.

Random inactivation of the X chromosome in female mammals represents a unique situation in which two distinct cell populations exist in the same individual. The pattern of X inactivation can be visualized by the insertion of a ubiquitous promoter-driven  $\beta$ -galactosidase reporter on the X chromosome (Reese et al., 1995). The critical role for proteins encoded by X-linked genes in a specific cellular compartment has been inferred by the extent of skewing of X-chromosome inactivation (Matthews et al., 1995; Hendriks et al., 1996). The fortuitous localization of the OCNC1 gene, essential for odorant-evoked activity in olfactory neurons, on the X chromosome provides a convenient model for directly examining the role of activity-dependent competition.

We have generated reporter-tagged OCNC1-deficient mice that permit a direct visualization of OCNC1-defi-

cient olfactory neurons and their projections. Male mice, in which all of the neurons are phenotypically mutant, retain the ability to generate a structurally normal olfactory epithelium and bulb. However, in heterozygous female mice, the population of OCNC1-deficient neurons is slowly depleted from the olfactory epithelium and displays an unusual pattern of projection to the olfactory bulb. Remarkably, this depletion of inactive, mutant cells is dependent on odorant exposure of the olfactory epithelium and can be reversed by odorant deprivation. These results suggest that odorant-evoked activity is crucial for olfactory neurons to survive in a competitive environment and implicate neuronal activity in the organization and maintenance of the olfactory system.

## Results

### Generation and Characterization of Reporter-Tagged OCNC1-Deficient Mice

Mice carrying a genetic disruption of the OCNC1 gene have been generated and characterized in several laboratories (Brunet et al., 1996; Parent et al., 1998; Baker et al., 1999; Lin et al., 2000; Zheng et al., 2000). These OCNC1-deficient animals are apparently normal at birth but display diminished weight gain and elevated neona-

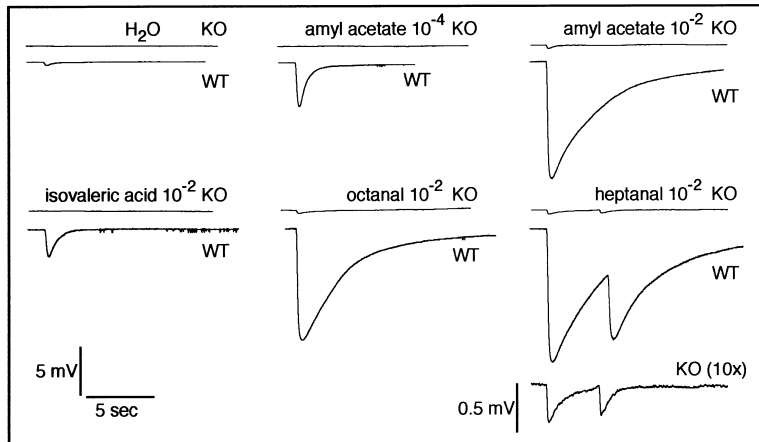


Figure 2. Odorant-Evoked Activity Is Essentially Eliminated in Tagged *OCNC1* Mutant Mice

EOG (electro-olfactogram) recordings were performed on 2-month-old mice. The top trace in each panel was from a *tau::lacZ*-tagged *OCNC1*<sup>-</sup> hemizygous male mouse (KO), and the lower trace was from a wild-type mouse (WT). Odorants were delivered in the vapor phase as 0.1 s pulse stimuli. The solution concentration ( $10^{-2}$ – $2 \times 10^{-2}$  M;  $10^{-4}$ – $1 \times 10^{-4}$  M) and the odorant are indicated in each panel. At  $2 \times 10^{-2}$  M, which is close to the saturating dose for EOG amplitude in wild-type mice, robust responses (for example, 14 mV for heptanal) were seen in wild-type animals, while these stimuli produced only small responses (0.4 mV for heptanal) in *OCNC1* mutant mice. In the bottom right, the small response seen for the KO in the double pulse paradigm has been scaled 10-fold to permit easier comparison to the WT response.

tal lethality. This lethality can be overcome by reduction in litter size and the surviving mutant animals approach the size and weight of wild-type littermates as they mature. We have generated two mouse lines in which the disrupted *OCNC1* allele has been tagged with the reporters *tau::lacZ* (a tau microtubule-associated protein- $\beta$ -galactosidase fusion protein) or *tau::EGFP* (tau-enhanced green fluorescent protein), respectively. These constructs facilitate the independent visualization of axon projection and cell fate of olfactory neurons expressing each of the tagged *OCNC1* mutant alleles.

The *OCNC1* gene replacement construct removed the region encoding amino acids 307 to the carboxyl terminus (amino acid 664) of the protein (Ruiz et al., 1996) (Figures 1A and 1B), including the conceptual pore domain and the cyclic nucleotide binding domain. This region was replaced with an IRES-*tau::lacZ* fragment (IRES, internal ribosomal entry site) or an IRES-*tau::EGFP* fragment and the resulting construct was introduced by homologous recombination into embryonic stem cells (Figures 1C and 1D). Transcription of this locus and IRES-directed translation of the *tau::lacZ* or *tau::EGFP* marker in mice should faithfully reflect the expression of the mutant *OCNC1* allele.

Histological examination of tissues from male mice

hemizygous for the X-linked, tagged *OCNC1* locus (*X<sup>OCNC1::tau-lacZ</sup>/Y*) revealed a structurally normal olfactory epithelium and bulb. Specifically, each of the characteristic cell types was present in olfactory epithelium, the olfactory neurons extended axons that fasciculated and projected to glomerular structures in the olfactory bulb. These observations were consistent with previous studies on untagged *OCNC1*<sup>(-/-)</sup> animals (Brunet et al., 1996; Parent et al., 1998; Baker et al., 1999; Lin et al., 2000; Zheng et al., 2000).

We next examined the expression of the *tau::lacZ* reporter in mutant male mice by histochemical staining for  $\beta$ -galactosidase activity. Whole mount preparations of olfactory epithelium revealed intense and uniform staining throughout the medial surface of the turbinates (Figure 1E) and on the septum. When the tissue was examined in cross section, staining was confined to olfactory neurons and the axon bundles residing beneath the epithelium (Figures 1F and 1G). The visualized olfactory axons covered the surface of the bulb and projected to underlying glomeruli (Figure 1H). Upon sectioning, the x-gal reaction product was generated throughout the olfactory nerve layer and in all glomeruli of the olfactory bulb (Figure 1I). Similar results were obtained in animals carrying the *tau::EGFP* marker (Figure 1J). In

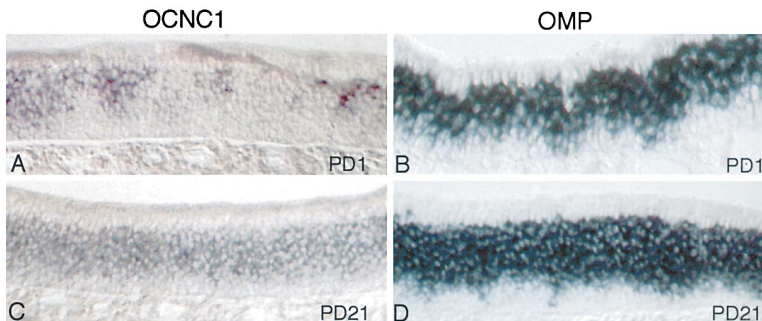
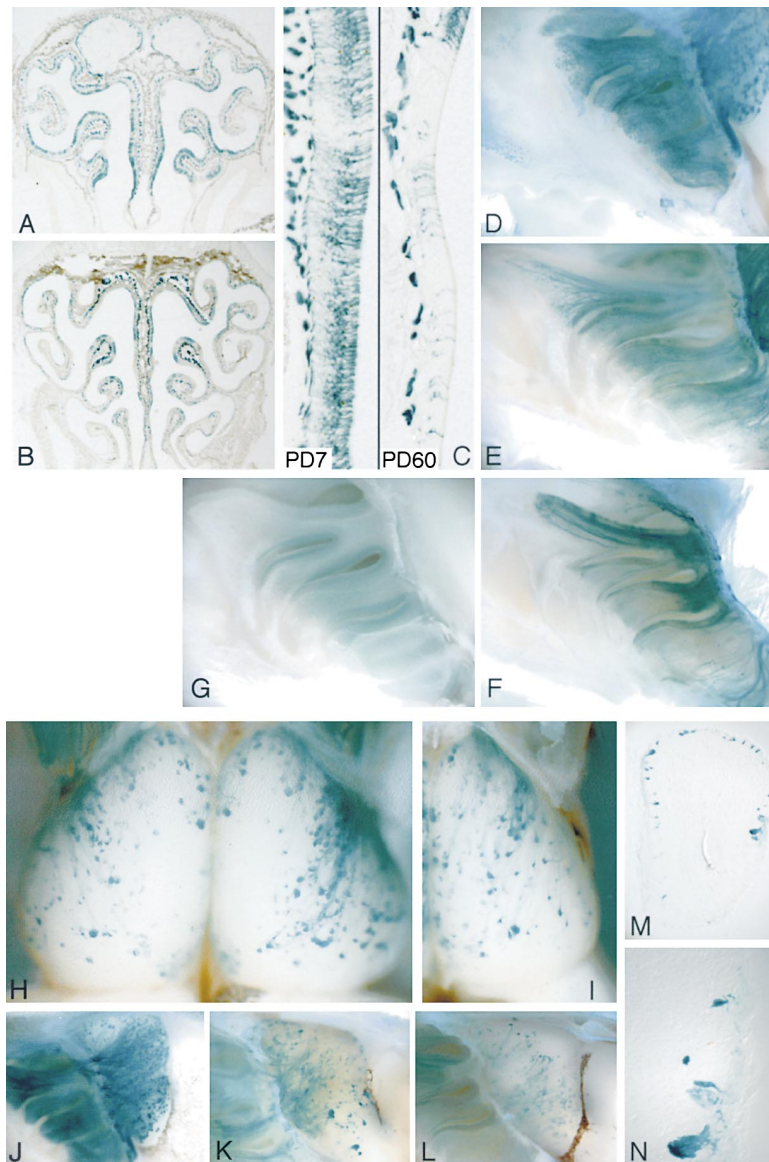


Figure 3. Distribution of *OCNC1*-Expressing Olfactory Neurons in Heterozygous Female Mice

In situ hybridization was performed in sections of olfactory epithelium from untagged *OCNC1*<sup>-</sup> heterozygous female mice at postnatal day (PD) 1 (A and B) and PD21 (C and D) using digoxigenin-labeled probes for *OCNC1* (A and C) and olfactory marker protein (OMP) message (B and D). In PD1 olfactory epithelium, areas of labeled (wild-type) and unlabeled (*OCNC1*-deficient) neurons are detected as patches of hybridization signal. At PD21, signal from wild-type cells appears uniform across the epithelium. Control hybridization for OMP mRNA reveals the distribution of all mature olfactory neurons.



**Figure 4. OCNC1-Deficient Olfactory Neurons Are Depleted from Olfactory Epithelium in Adult *OCNC1*<sup>-/+</sup> Heterozygous Female Mice**

(A–F) X-gal staining of the olfactory epithelium of *tau::lacZ*-tagged *OCNC1*<sup>-/+</sup> heterozygous female mice. (A) A coronal section of olfactory epithelium at postnatal day (PD) 7 stained with x-gal. (B) A stained coronal section of olfactory epithelium at 2 months. (C) High magnification of the septum from PD7 and PD60 mice. Individual stained cells can be seen in the epithelium. (D, E, and F) Whole mount views of the medial surface of nasal turbinates from mice at PD7 (D); 2 months (E); and 1 year (F). (G) Whole mount view of the medial surface of nasal turbinates in a wild-type mouse.

(H–N) X-gal staining of the olfactory bulbs of *tau::lacZ*-tagged *OCNC1*<sup>-/+</sup> heterozygous female mice. (H) Dorsal view of olfactory bulbs from a 2-month-old mouse in whole mount. (I) Right olfactory bulb of a different 2-month-old mouse. (J, K, and L) Whole mount views of the medial surfaces of olfactory bulb from mice at PD7 (J); 2 months (K); and 1 year (L). (D) and (J) are from the same mouse, so are (E) and (K). (M and N) A coronal section from a 2-month-old mouse in low (M) and high (N) magnification. At PD7, the staining is seen in a large number of glomeruli in olfactory bulb, while in adult mice, only a fraction of the glomeruli are x-gal positive, most glomeruli lack blue staining.

each case, the observed reporter expression was consistent with the *OCNC1* expression pattern previously published (Brunet et al., 1996; Parent et al., 1998). We therefore conclude that the expression of *tau::lacZ* or *tau::EGFP* accurately reflects the expression of *OCNC1* gene.

We then used electro-olfactogram (EOG) recording (Ottoson, 1971) to confirm the disruption of *OCNC1* function in tagged *OCNC1*-deficient animals (Figure 2). We performed EOG analysis on adult mouse epithelium and delivered odorants in the vapor phase from known solution concentrations. Amyl acetate evoked a dose-dependent response in wild-type animals ( $10^{-4}$  M and  $2 \times 10^{-2}$  M in figure 2). The higher concentration was close to the saturating dose for EOG amplitude in wild-type mice. At  $2 \times 10^{-2}$  M, wild-type mice generated a robust response to each of the eight odorants tested. In contrast, *OCNC1*-deficient mice ( $n = 3$ ) displayed no detectable responses to amyl acetate at  $10^{-4}$  M and only a very small but reproducible response to each of the

odorants except isovaleric acid at  $2 \times 10^{-2}$  M. A dual-pulse paradigm revealed a similar response pattern and desensitization extent as in wild-type animals and further supported the validity of these responses (Figure 2). The origin and physiological significance of these trace responses recorded at odorant concentrations much higher than animals encounter in the environment is unclear. Nevertheless, these results showed that the tagged disruption of the *OCNC1* gene resulted in essentially complete elimination of odorant-evoked activity in the olfactory epithelium.

#### **OCNC1-Deficient Olfactory Neurons Are Depleted in Adult Heterozygous Females**

The presence of a morphologically normal olfactory epithelium in male hemizygous *OCNC1*-deficient mice suggested that the epithelium of heterozygous female animals would consist of a mosaic of wild-type and mutant olfactory neurons. The distribution of these cells would reflect the random inactivation of the two X chromo-

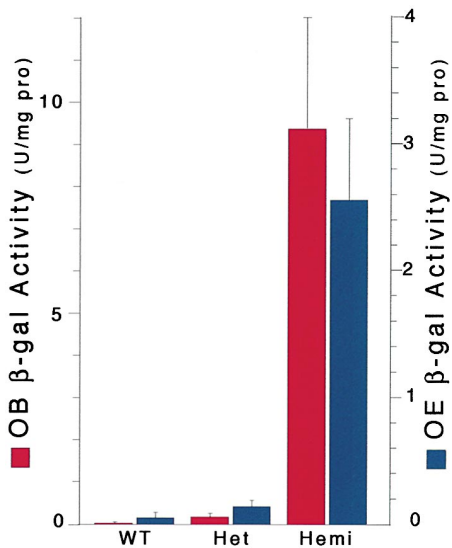


Figure 5. Quantitative Assay of  $\beta$ -Galactosidase Activity in tau::lacZ-Tagged Adult Mice

Enzyme activity was determined in tissue homogenates from olfactory epithelium (OE, blue) and olfactory bulb (OB, red) of wild-type (WT), heterozygous female (Het), and hemizygous male (Hemi) mice. Activity levels were: OE, WT = 0.03  $\pm$  0.02 (mean  $\pm$  SD); Het = 0.18  $\pm$  0.08; Hemi = 9.37  $\pm$  2.62. In OB, WT = 0.06  $\pm$  0.02; Het = 0.15  $\pm$  0.03; Hemi = 2.57  $\pm$  0.66. Each data point represents the independent assessment of tissues from at least four animals.

some in the progenitor population and the migration of cells during maturation. Surprisingly, *in situ* hybridization using an OCNC1 probe (Parent et al., 1998) on adult heterozygous female mice carrying one untagged, OCNC1-deleted allele (Parent et al., 1998) revealed that the wild-type OCNC1 message was expressed by apparently all of the mature olfactory neurons (Figure 3C). In contrast, the olfactory epithelium of neonatal animals consisted of both wild-type (labeled) and OCNC1-deficient (unlabeled) olfactory neurons arranged in distinct domains (Figure 3A). Mature olfactory neurons were present throughout the epithelium at each time point (Figures 3B and 3D). These observations indicated that the OCNC1-deficient olfactory neurons were depleted in adult heterozygous females. Unfortunately, *in situ* hybridization marks the wild-type cells and provides only an indirect assessment of the OCNC1-deficient cell population. We therefore utilized the tagged OCNC1<sup>-</sup> allele in heterozygous female animals to directly visualize the OCNC1-deficient neurons in olfactory epithelium and their projections in olfactory bulb.

The distribution of OCNC1-deficient cells in olfactory epithelium was examined by  $\beta$ -galactosidase staining of tissue from postnatal day (PD) 7 and adult female heterozygous animals ( $n \geq 8$  for each group) (Figure 4). At PD7, the epithelium is still undergoing rapid expansion and the organization of the olfactory bulb has been defined. Distinct regions of unstained cells (wild-type) and cells expressing the OCNC1 mutant allele could be visualized in coronal sections and in whole mount preparations by virtue of the  $\beta$ -galactosidase expression (Figures 4A, 4C left panel, and 4D). The blue staining was robust but patchy throughout the epithelium. In the

epithelium of adult mice (Figures 4B, 4C right panel, and 4E), the blue-stained OCNC1-deficient neurons, which were randomly distributed in patchy clusters or as individual cells, were both fewer in number and occupied a smaller extent of the epithelium. In animals over 1-year-old, x-gal staining was only faint or absent in most areas of the epithelium with a small number of labeled olfactory neurons (Figure 4F).

Olfactory neurons stochastically express a particular odorant receptor and converge to a single glomerulus within the olfactory bulb. Thus, axons converging to each glomerulus would be expected to derive from a mixture of the phenotypically OCNC1(+) and OCNC1(-) cells within the epithelium. Interestingly, only a subset of the olfactory glomeruli were x-gal positive and these were distributed across the bulb surface in adult heterozygous females (Figures 4H, 4I, 4K, and 4L). This result was in marked contrast to the uniform staining of glomeruli observed in adult male hemizygous mice (Figure 1H) and to a large number of stained glomeruli visible in the olfactory bulb of PD7 animals (Figure 4J). In heterozygous adult females, approximately 100 to 500 stained glomeruli ( $n = 10$  animals) were observed out of about the 1800 total glomeruli in the mouse (Royet et al., 1988). There was considerable variability in the number of stained glomeruli from animal to animal and more modest variation between the two bulbs of a given animal. In spite of these variations, many stained glomeruli were apparently in bilaterally symmetrical positions (Figure 4H) and their positions displayed some conservation between animals (Figures 4H and 4I). Further support for these observations will require complete serial reconstruction and complex morphometric analysis of the olfactory bulb.

When the olfactory bulb was sectioned prior to x-gal staining, it was possible to detect individual sensory fibers and determine whether most stained glomeruli received input from multiple olfactory neurons. OCNC1-deficient cells innervate only a fraction of the glomeruli (Figure 4M). At higher magnification (Figure 4N), we observed multiple fibers that innervated the stained regions while most of the glomeruli were devoid of any x-gal-positive axons. These results suggest that olfactory neurons differ in their ability to innervate particular glomeruli, perhaps reflecting the differences in their receptor identity and odorant responsiveness.

To assess the depletion of OCNC1-deficient olfactory neurons in adult heterozygous animals, we measured  $\beta$ -galactosidase activity in tissue homogenates (Figure 5). The enzymatic activity in epithelial extracts from hemizygous males was dramatically higher than the basal activity observed in wild-type animals. In heterozygous females,  $\beta$ -galactosidase activity in the epithelium was only 6% of that seen in males (Figure 5). These differences reflect the reduction in the number of OCNC1-deficient cells and decreased staining throughout the epithelium. Enzyme activity in the olfactory bulb, derived from tau::lacZ translocation of epithelium-expressed protein, displayed a similar pattern.

We conclude that OCNC1-deficient neurons are generated and are competent to project axons into the olfactory bulb during postnatal development. However, the presence of mutant and wild-type cells in the same epi-

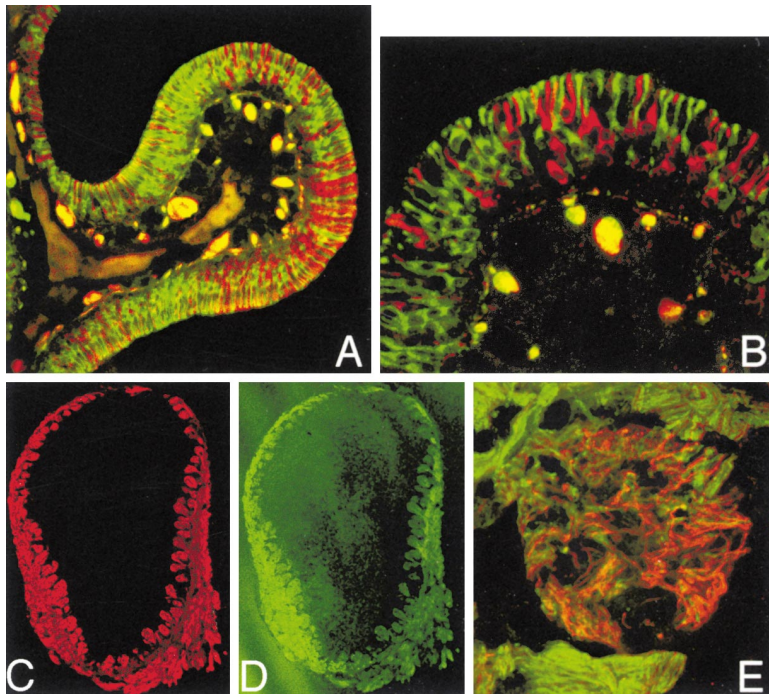


**Figure 6. Random X Inactivation of Reporter-Tagged Alleles in *OCNC1*-Deficient Homozygous Female Mice**

Cryosections from the double-tagged *OCNC1*<sup>-/-</sup> homozygous female mice, with one allele tagged with *tau::lacZ* and another allele marked with *tau::EGFP*, were examined by confocal microscope for β-galactosidase and GFP expression. β-Galactosidase was visualized with anti-β-gal antibody and a Cy3-conjugated secondary in the red channel and EGFP was detected by intrinsic green fluorescence. (A and B) Olfactory epithelium at low (A) and high (B) magnification. The red- and green-labeled olfactory neurons are distributed in patches (A), but extensive mingling of individual cells is observed in the epithelium (B) where each olfactory neuron is labeled exclusively by either the red (β-gal) or green (EGFP) reporter. Axon bundles residing beneath the epithelium contain a mixture of labeled fibers (B), but some segregation of fibers is apparent. In a coronal section of olfactory bulb, staining for β-galactosidase in (C) and intrinsic GFP fluorescence in (D) reveals that all glomeruli are labeled. Both red and green fluorescence exist throughout the olfactory nerve layer and are in all glomeruli. A high magnification view of a single olfactory glomerulus (E) reveals that separate red- and green-labeled single fibers can be distinguished.

thelium leads to dramatically reduced survival of the *OCNC1*-deficient neurons in these mosaic animals.

**Both Reporter-Tagged *OCNC1* Alleles Are Expressed in *OCNC1*-Deficient Homozygous Females**

We hypothesized that depletion of *OCNC1*-deficient olfactory neurons in adult heterozygous females arose from a competition between wild-type and *OCNC1*-deficient neurons. If the two X chromosomes in female mice were tagged with different reporters, a noncompetitive condition should result and two distinct populations of neurons in the epithelium would be retained even in adult mice. We therefore generated double-tagged *OCNC1*<sup>-/-</sup> homozygous female mice where one allele was tagged with *tau::lacZ* and another allele was marked with *tau::EGFP*.

Individual olfactory neurons from *OCNC1*<sup>-</sup> *tau::lacZ*/*OCNC1*<sup>-</sup> *tau::EGFP* mice express exclusively either *lacZ* (visualized with a Cy3-labeled antibody) or GFP (Figures 6A and 6B), thereby confirming that this locus is subject to X inactivation. The patches of *lacZ*-positive and GFP-positive neurons are clearly visible (Figure 6A) and reflect the mosaic organization of the tissue. However, these clusters of olfactory neurons are not exclusive, cells expressing each marker are intermingled in the neuronal layer of the epithelium (Figure 6B). This contrasts with retinal photoreceptor cell generation (Reese et al., 1995) and suggests that considerable mixing of stem cells occurs early in development of the tissue or alternatively arises from migration of dividing progenitors or developing neurons. Moreover, the numbers of *lacZ* neurons and GFP neurons in olfactory epithelium

are roughly equal, demonstrating that in an adult female mouse, the two differentially tagged, *OCNC1*-deficient neurons can coexist in the epithelium.

Every glomerulus in double-tagged *OCNC1*<sup>-/-</sup> mice would be expected to receive innervation from cells expressing each of the reporters. The coincidence of the two signals is apparent with all glomeruli containing fibers derived from both *lacZ*-expressing and GFP-expressing cells (Figures 6C and 6D). Although these fibers were intermingled in the fasciculated axon bundles, independently labeled single fibers were readily observed in the neuropil of the glomerulus (Figure 6E).

**Depletion of *OCNC1*-Deficient Neurons Is Dependent on Odorant-Evoked Activity**

The known role of the *OCNC1* channel subunit in sensory transduction suggested that the absence of odorant-evoked activity contributed to depletion of the *OCNC1*-deficient olfactory neurons in adult heterozygous female mice. Blockade of odorant stimulation might spare the *OCNC1*-deficient neurons since under these conditions the level of evoked activity in wild-type neurons would decline to that of the *OCNC1*-deficient cells. We therefore performed unilateral naris occlusion on *tau::lacZ*-tagged animals shortly after birth and examined the epithelium and bulb 40 days to 4 months later. Olfactory neurons project ipsilaterally to the bulb and the unoccluded naris provided the control tissue for each animal.

In *OCNC1* heterozygous female mice (n = 14), x-gal staining revealed a dramatic difference between the naris-occluded side and the untreated side in both olfactory epithelium and olfactory bulb (Figure 7). Many more x-gal-reactive neurons were present on the occluded

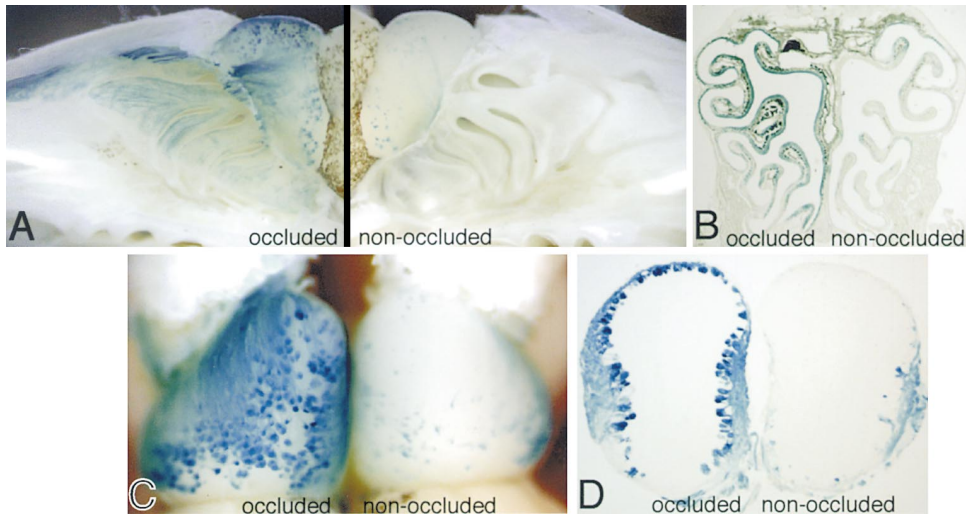


Figure 7. Blocking of Odor Stimulation by Naris Occlusion Prevents the Depletion of OCNC1-Deficient Olfactory Neurons in *OCNC1*<sup>+/-</sup> Heterozygous Female Mice

Unilateral naris occlusion was performed on PD1–5 mice and  $\beta$ -galactosidase expression in olfactory tissue of heterozygous females examined 40 days to 4 months post treatment. The naris occlusion blocked the odor stimulation of olfactory neurons on the ipsilateral side (always shown on the left).

(A) Whole mount views of the medial surface of nasal turbinates and olfactory bulbs of both naris-occluded side (left) and the untreated side (right). The paired image is flipped to correspond to the image displayed in (C).

(B) Coronal section of olfactory epithelium. Septum divides the occluded side from the control, odor-exposed nasal cavity.

(C) A dorsal view of the olfactory bulb in whole mount from the same animal as in (A).

(D) Coronal section of the olfactory bulb. Extensive innervation by x-gal-positive axons is apparent on the occluded side. Data are representative of observations in 14 animals.

side than on the untreated side (Figures 7A and 7B). The extent of this OCNC1-deficient neuronal rescue by naris occlusion was assessed in 10  $\mu$ m coronal sections of an animal. Along the septum, 130 cells/mm were x-gal positive on the open side and this number was increased 4.5-fold to 570 cells/mm on the occluded side. The olfactory bulb also contained many more blue-labeled glomeruli and more intense staining on the side receiving input from the occluded naris (Figures 7A, 7C, and 7D). The number of stained glomeruli on the activity-blocked side of some animals approached that seen in homozygous male mice (Figure 1H) although the intensity of staining was reduced. In five coronal sections (20  $\mu$ m, 300 to 400  $\mu$ m intervals) of an olfactory bulb from the open side, only 18% (73/404) of glomeruli were labeled (5% to 29% range), while on the occluded side, 70% (318/455) were x-gal positive (range 59% to 78%). Results obtained from animals with unilateral naris closure for 40 days to 4 months were similar. Odorants entering the nasal cavity through the oral cavity could contribute to the regional variation in depletion and allow residual odorant exposure to the sensory epithelium.

These results strongly indicate that the depletion of OCNC1-deficient olfactory neurons in adult heterozygous females is dependent on odorant-evoked activity. It further suggests that evoked activity contributes to olfactory neuron survival in a competitive environment.

## Discussion

We have utilized a molecular genetic approach to explore the contribution of stimulus-evoked activity in ol-

factory system development and maintenance. The unique role of the OCNC1 channel subunit in the transduction of sensory information and the location of the gene encoding this protein on the X chromosome provides an opportunity to dissect aspects of activity-dependent function that were not obvious in physiological or morphological analysis of animals carrying simple gene disruptions. These studies have revealed an unanticipated role for activity-dependent competition in the survival of olfactory neurons.

## Mechanism of Olfactory Neuron Depletion

How are OCNC1-deficient neurons depleted from the epithelium in heterozygous mice? The contribution of activity to sensory neuronal development has been established and it is tempting to speculate that related processes operate in the olfactory system. However, the unique capacity of olfactory neurons to undergo continual replacement from basal cells throughout life allows for additional mechanisms. Consider, for example, a situation where OCNC1-deficient neurons and their progenitors were normal in proliferation, differentiation, and connectivity with the bulb but displayed a significantly shorter lifespan. Over time, the epithelium would be populated by an increasing number of wild-type cells as mutant cells were preferentially lost and replaced randomly by wild-type or mutant cells. This would be a self-limiting process regulated by the relative lifetimes of the two populations. Such a population of the tagged mutant cells would be expected to project to all glomeruli and would not produce the results seen here.

In olfactory epithelium, trophic factors and their re-

ceptors are likely to play an important role in regulating the number of mature olfactory neurons and their survival (Roskams et al., 1996). In other systems, survival is dependent on trophic factors supplied in limited amounts by target cells (Oppenheim, 1991). The requirement of depolarization for uptake of extrinsic factors can account for the selective survival of electrically active cells (Ghosh et al., 1994). Odorant-evoked activity may provide differentiating olfactory neurons an enhanced capacity (in comparison to their less active peers) to acquire essential neurotrophic factors. In *OCNC1*<sup>-/+</sup> heterozygous mice, the odorant-activated, wild-type neurons would have an advantage for acquiring neurotrophic factors and thus lead to depletion of *OCNC1*-deficient cells from the differentiating population. When evoked activity is abrogated by naris occlusion, wild-type and mutant neurons would acquire trophic factors on a more equal basis and *OCNC1*-deficient neurons as well as wild-type neurons would both be resident in the epithelium. In principle, this differential survival could involve processes intrinsic to the epithelium, but an olfactory bulb origin of these factors seems more likely.

#### Role of Evoked Activity in Development and Organization of the Olfactory System

It is likely that the number of synapses and the size of individual glomeruli are highly regulated. In *OCNC1*<sup>-/+</sup> heterozygous mice, the dramatic effect of evoked activity is revealed by the existence of two extreme cell types, fully active normal cells and inactive mutant cells. Even when all cells are equivalent, activity-dependent competition between wild-type neurons could contribute to determine the number of olfactory neurons of particular receptor specificities and the size of glomeruli in olfactory bulb.

Olfactory neurons expressing the same odorant receptor at different levels likely display distinct thresholds for odorant-evoked activity and ability to compete for the same glomerulus. Several reports have suggested that receptors expressed from genetically altered loci project to subdomains within a glomerulus or to distinct glomeruli-like structures (Royal and Key, 1999; Gogos et al., 2000; Zheng et al., 2000). Perhaps it is the level of odor-evoked activity rather than the level of receptor protein that contributes to this segregation of fibers. Examination of the projection patterns of specifically tagged receptor neurons in an activity-deficient background would clarify the origins of these aberrant glomeruli. Evolutionarily, mutations in receptors that result in altered odorant activation profiles would simultaneously eliminate these fibers from their original target and allow them to assemble into distinct glomeruli.

#### Retention of Stereotyped Stained Glomeruli in Heterozygous Female Mice

The stereotyped, persistent innervation of some glomeruli in the olfactory bulb by *OCNC1*-deficient neurons (Figures 4H and 4I) suggested that competition mechanisms are not uniformly effective for determining the survival of neurons expressing different receptors. These differences could reflect variation in the intrinsic properties of individual glomeruli or environmental factors.

Specifically, the laboratory odors determine the activity in neurons expressing different receptors and converging to distinct glomeruli. If the odor environment lacks effective stimuli for a particular odorant receptor, the *OCNC1*-deficient neurons expressing that receptor would not be subject to activity-dependent elimination and their stereotyped connections would persist. The glomeruli with no blue staining would identify sites that are activated by environmental odorants while blue-stained glomeruli would represent those sites that receive innervation from receptor neurons that recognize odors not present in the environment. This process is recapitulated globally in the naris occlusion experiments where the effective elimination of environmental odorant exposure allows all glomeruli to be innervated by *OCNC1*-deficient neurons (Figure 7). Moreover, our results suggest that most glomeruli receive inputs from receptor neurons that are subject to evoked activity in the laboratory environment.

Recently, the role of *OCNC1*-mediated activity in targeting of neurons expressing two different receptors was examined (Lin et al., 2000; Zheng et al., 2000). The different effects of *OCNC1* expression on the projection of neurons expressing the M72 and P2 receptors might reflect the presence or absence of ligands for these receptors in the odor environment rather than intrinsic properties of the receptors or the glomeruli that they innervate. It would be interesting to examine specific receptors in this system, especially if their cognate ligands were known.

#### Contribution of Other Signaling Mechanisms to Odorant Detection

The residual activity observed in EOG recordings from adult, tagged *OCNC1*-deficient mice (Figure 2) contrasts with the reported complete lack of EOG response to odors in neonatal (Brunet et al., 1996) and embryonic (Lin et al., 2000) animals carrying similar disruptions of the *OCNC1* gene. It is highly unlikely that a truncated protein lacking the pore region, sixth transmembrane domain, and the cyclic nucleotide binding domain of the *OCNC1* protein, if made, would associate with the *OCNC2* and  $\beta$  subunits or form a functional channel. Rather, the larger EOG responses we obtained in recordings from adult animals might account for our ability to observe these responses. The small signals recorded at a high concentration of odorants are not likely to be an artifact since their pattern closely mimics the native responses, even in a double-pulse stimulation paradigm (Figure 2). The remaining cyclic nucleotide channel subunits, *OCNC2* and the  $\beta$  subunit, could form a channel activated by other second messengers (Broillet and Firestein, 1997) or by the elevated cAMP concentrations achieved at high odorant concentrations. Alternatively, other signaling pathways (Boekhoff et al., 1990; Juiffs et al., 1997) might mediate responses to some odors. Further elucidation of the signaling mechanisms responsible for these responses will require additional genetic and physiological characterization.

#### General Application of X Inactivation to Analysis of Gene Function

The generation of animals containing two distinct cell populations has proven to be a powerful tool in elucidat-

ing cell lineage and allowing partial rescue of homozygous lethality. The generation of genetic mosaics in *Drosophila* and ES cell-generated chimeric mice provides individual animals for study but, unfortunately, this mosaicism is not propagated through the germline. In mammals, X chromosome inactivation in females shortly after implantation represents one mechanism to generate large numbers of mosaic animals. In some situations, the presence of a wild-type cell population will overcome developmental lethality and allow the isolation and characterization of differentiated mutant cells. Alternatively, the presence of tissue-specific skewing of X inactivation has been used in some systems to reveal the critical site of action of a cell-autonomous gene (Hendriks et al., 1996). Finally, the competition between two distinct cell populations as described here is a powerful tool to reveal subtle (and not so subtle) defects that are obscured in traditional knockouts due to partial genetic redundancy or ability of the defective system to establish adequate function.

Although the presence of the *OCNC1* gene on the X chromosome simplified our experiments, in principle this methodology could be applied to autosomal genes. Specifically, complementation of gene disruptions on an autosome with tagged alleles introduced onto the X chromosome can generate chimeric heterozygous female animals. The introduction of a single functional gene at a defined location on the X chromosome will create a competitive condition in a background where the autosomal alleles are mutated. The number and nature of the alleles introduced onto the X chromosome (mutant versus wild-type) will depend on the experimental design but the availability of efficient methods for introducing large DNA constructs at defined sites makes these approaches tractable.

## Experimental Procedures

### Gene Targeting

A 9.6 kb DNA fragment containing the *OCNC1* gene (Ruiz et al., 1996) was used to construct the gene disruption construct. A 1244 bp *HincII*-*HindIII* portion encoding amino acids 307–664(COOH) of the protein and a 170 bp 3' untranslated region were replaced with sequences encoding an IRES-tau::LacZ(ETL) (IRES, internal ribosomal entry site) or an IRES-tau::EGFP (ETG) reporter. The targeting vectors were modified versions of ETLpA(-)/LNTL (IRES-tau::LacZ/loxP-tk-neo-loxP) (Mombaerts et al., 1996), in which a 476 bp fragment (*BstBI*-*NruI*) of the thymidine kinase (*tk*) gene was deleted to permit transmission through the male germline (Braun et al., 1990). The fragment containing the reporter and selectable marker were flanked by *OCNC1* homology regions of 4 kb (3' arm) (Parent et al., 1998) and 3.85 kb (5' arm). ETLpA(-)/LNL was constructed by replacing the 3 kb *BamHI*-*BamHI* lacZ-containing fragment of ETLpA(-)/LNL with a 0.75 kb EGFP fragment (*BamHI*-*XbaI*) from plasmid pEGFP-N1 (CLONTECH Palo Alto, CA). Linearized constructs were electroporated into 129/Sv embryonic stem (ES) cells and homologous recombination events were identified by Southern blot analysis. The genetically modified ES cells were injected into C57BL/6 blastocysts and germline transmission of the reporter assessed after crossing the resulting chimeric males with *cre*-transgenic female mice (Schwenk et al., 1995).

### Expression Patterns

In situ hybridization to visualize the expression of the *OCNC1* mRNA was performed with a digoxigenin-labeled 0.75 kb *HindIII* sequence not present in the mutant allele (Parent et al., 1998). The coding region of *OMP* gene was used as the control probe. The in situ

hybridization was performed essentially as described (Schaeren-Wiemers and Gerfin-Moser, 1993).

The x-gal staining for whole mount preparation and on sections was performed as described by Mombaerts et al. (Mombaerts et al., 1996) with overnight incubation. Tissues were isolated following an overdose of mice with ketamine-xylazine (RBI, Natick, MA) and intracardiac perfusion with either 4% paraformaldehyde or 2% paraformaldehyde plus 0.25% glutaraldehyde in PBS (pH 7.4) for 10 min. For whole mount visualization of reporter expression, olfactory epithelium and olfactory bulb were then dissected, washed with PBS, and stained. For cryosections, dissected tissues were treated with 20% sucrose plus 250 mM EDTA for 24 hr at 4°C, frozen in OCT compound (Sukura Finetek, Torrance, CA), and cut at 10–20  $\mu$ m in a cryostat.

### EOG Recording

The instrumentation, animal preparation, odorant stimulus delivery, and data analysis for electro-olfactogram (EOG) recording closely followed described procedures (Zhao et al., 1998). Stock solutions of odorants (0.5 M in DMSO) were diluted in water to the indicated concentrations. Vapor-phase odorant stimuli were generated by placing 2 ml of solution in a 10 ml glass test tube and allowing the air above the solution to equilibrate with the odorant. This vapor was delivered as a 0.1 s pulse injected into a continuous stream of humidified air flowing over the tissue sample. The EOGs were initially recorded using amyl acetate at  $10^{-4}$  M,  $10^{-3}$  M, and  $2 \times 10^{-2}$  M. Seven additional odorants ((-)-carvone; cineole; citral; hexanal; heptanal; isovaleric acid; octanal) were then tested at  $2 \times 10^{-2}$  M. The magnitudes of EOG responses were normalized by scaling the response to  $10^{-4}$  M (wild-type) or  $2 \times 10^{-2}$  M amyl acetate (*OCNC1*-deficient) at several points in the experiment to the initial response to the amyl acetate reference. All odorants were purchased from Aldrich.

### $\beta$ -Galactosidase Activity Assay

The  $\beta$ -galactosidase activity in olfactory tissue was assessed in homogenates using the  $\beta$ -galactosidase enzyme assay system (Promega, Madison, WI). Samples of olfactory epithelium (with septal and turbinate bone) and olfactory bulb were dissected, homogenized in the lysis buffer provided, and aliquots were stored at  $-80^{\circ}\text{C}$ . The protein concentration of sample was determined by using protein assay reagent (BioRad, Hercules, CA).

### Immunohistostaining

Tissue sections were incubated with rabbit antisera to  $\beta$ -galactosidase (Eppendorf-5 Prime, Boulder, CO) at 1:1500 dilution in TBST (10 mM Tris, 150 mM NaCl, 0.1% Triton X-100) containing 1% normal donkey serum. After washing, the sections were reacted with Cy3-conjugated donkey anti-rabbit antibody (1:200) from Jackson ImmunoResearch Laboratories (West Grove, PA) and imaged by confocal microscopy.

### Naris Occlusion

Animals of 1 to 5 days postnatal age were cooled briefly to anesthetize and one nostril was lightly cauterized with a fine tip surgical cautery (Henley International, TX). The pups were returned to their cage. Scar formation leads to naris closure that was confirmed by stereoscopic visual examination at time of tissue harvest.

### Acknowledgments

We appreciate the invaluable guidance and assistance of Yanshu Wang in generating knockouts, Peter Mombaerts and Stephen Munger for DNA constructs, Karen Schrader for technical assistance, and Mitra Cowan at Transgenic Facility of Johns Hopkins Medical School. King-Wai Yau and Weihong Xiong contributed to EOG recording design and data analysis, and members in the laboratory provided stimulating discussions. This research was supported by Howard Hughes Medical Institute and by a grant from the National Institutes of Health (NIDCD) to R. R. R.

Received November 27, 2000; revised January 16, 2001.

## References

- Baker, H. (1990). Unilateral, neonatal olfactory deprivation alters tyrosine hydroxylase expression but not aromatic amino acid decarboxylase or GABA immunoreactivity. *Neuroscience* 36, 761–771.
- Baker, H., Cummings, D.M., Munger, S.D., Margolis, J.W., Franzen, L., Reed, R.R., and Margolis, F.L. (1999). Targeted deletion of a cyclic nucleotide-gated channel subunit (OCNC1): biochemical and morphological consequences in adult mice. *J. Neurosci.* 19, 9313–9321.
- Boekhoff, I., Tareilus, E., Strotmann, J., and Breer, H. (1990). Rapid activation of alternative second messenger pathways in olfactory cilia from rats by different odorants. *EMBO J.* 9, 2453–2458.
- Braun, R.E., Lo, D., Pinkert, C.A., Widera, G., Flavell, R.A., Palmiter, R.D., and Brinster, R.L. (1990). Infertility in male transgenic mice: disruption of sperm development by HSV-tk expression in postmeiotic germ cells. *Biol. Reprod.* 43, 684–693.
- Broillet, M.C., and Firestein, S. (1997). Beta subunits of the olfactory cyclic nucleotide-gated channel form a nitric oxide activated Ca<sup>2+</sup> channel. *Neuron* 18, 951–958.
- Brunet, L.J., Gold, G.H., and Ngai, J. (1996). General anosmia caused by a targeted disruption of the mouse olfactory cyclic nucleotide-gated cation channel. *Neuron* 17, 681–693.
- Brunjes, P.C. (1994). Unilateral naris closure and olfactory system development. *Brain Res. Brain Res. Rev.* 19, 146–160.
- Chess, A., Simon, I., Cedar, H., and Axel, R. (1994). Allelic inactivation regulates olfactory receptor gene expression. *Cell* 78, 823–834.
- Cummings, D.M., and Brunjes, P.C. (1994). Changes in cell proliferation in the developing olfactory epithelium following neonatal unilateral naris occlusion. *Exp. Neurol.* 128, 124–128.
- Farbman, A.I. (1992). *Cell Biology of Olfaction* (New York: Cambridge University Press).
- Farbman, A.I., Brunjes, P.C., Rentfro, L., Michas, J., and Ritz, S. (1988). The effect of unilateral naris occlusion on cell dynamics in the developing rat olfactory epithelium. *J. Neurosci.* 8, 3290–3295.
- Fawcett, J.W., O'Leary, D.D., and Cowan, W.M. (1984). Activity and the control of ganglion cell death in the rat retina. *Proc. Natl. Acad. Sci. USA* 81, 5589–5593.
- Frazier, L.L., and Brunjes, P.C. (1988). Unilateral odor deprivation: early postnatal changes in olfactory bulb cell density and number. *J. Comp. Neurol.* 269, 355–370.
- Ghosh, A., Camahan, J., and Greenberg, M.E. (1994). Requirement for BDNF in activity-dependent survival of cortical neurons. *Science* 263, 1618–1623.
- Gogos, J.A., Osborne, J., Nemes, A., Mendelsohn, M., and Axel, R. (2000). Genetic ablation and restoration of the olfactory topographic map. *Cell* 103, 609–620.
- Graziadei, P.P., and Graziadei, G.A. (1979). Neurogenesis and neuron regeneration in the olfactory system of mammals. I. Morphological aspects of differentiation and structural organization of the olfactory sensory neurons. *J. Neurocytol.* 8, 1–18.
- Hendriks, R.W., de Bruijn, M.F., Maas, A., Dingjan, G.M., Karis, A., and Grosveld, F. (1996). Inactivation of Btk by insertion of lacZ reveals defects in B cell development only past the pre-B cell stage. *EMBO J.* 15, 4862–4872.
- Juilfs, D.M., Fulle, H.J., Zhao, A.Z., Houslay, M.D., Garbers, D.L., and Beavo, J.A. (1997). A subset of olfactory neurons that selectively express cGMP-stimulated phosphodiesterase (PDE2) and guanylyl cyclase-D define a unique olfactory signal transduction pathway. *Proc. Natl. Acad. Sci. USA* 94, 3388–3395.
- Katz, L.C., and Shatz, C.J. (1996). Synaptic activity and the construction of cortical circuits. *Science* 274, 1133–1138.
- LeVay, S., Wiesel, T.N., and Hubel, D.H. (1980). The development of ocular dominance columns in normal and visually deprived monkeys. *J. Comp. Neurol.* 191, 1–51.
- Lin, D.M., Wang, F., Lowe, G., Gold, G.H., Axel, R., Ngai, J., and Brunet, L. (2000). Formation of precise connections in the olfactory bulb occurs in the absence of odorant-evoked neuronal activity. *Neuron* 26, 69–80.
- Mackay-Sim, A., and Kittel, P. (1991). Cell dynamics in the adult mouse olfactory epithelium: a quantitative autoradiographic study. *J. Neurosci.* 11, 979–984.
- Malnic, B., Hirono, J., Sato, T., and Buck, L.B. (1999). Combinatorial receptor codes for odors. *Cell* 96, 713–723.
- Matthews, P.M., Benjamin, D., Van Bakel, I., Squier, M.V., Nicholson, L.V., Sewry, C., Barnes, P.R., Hopkin, J., Brown, R., Hilton-Jones, D., et al. (1995). Muscle X-inactivation patterns and dystrophin expression in Duchenne muscular dystrophy carriers. *Neuromuscul. Disord.* 5, 209–220.
- Mombaerts, P., Wang, F., Dulac, C., Chao, S.K., Nemes, A., Mendelsohn, M., Edmondson, J., and Axel, R. (1996). Visualizing an olfactory sensory map. *Cell* 87, 675–686.
- Oppenheim, R.W. (1991). Cell death during development of the nervous system. *Annu. Rev. Neurosci.* 14, 453–501.
- Ottoson, D. (1971). The electro-olfactogram. In *Handbook of Sensory Physiology (Olfaction)*, L.M. Beidler, ed. (Berlin: Springer-Verlag), pp. 95–131.
- Parent, A., Schrader, K., Munger, S.D., Reed, R.R., Linden, D.J., and Ronnett, G.V. (1998). Synaptic transmission and hippocampal long-term potentiation in olfactory cyclic nucleotide-gated channel type 1 null mouse. *J. Neurophysiol.* 79, 3295–3301.
- Reese, B.E., Harvey, A.R., and Tan, S.S. (1995). Radial and tangential dispersion patterns in the mouse retina are cell-class specific. *Proc. Natl. Acad. Sci. USA* 92, 2494–2498.
- Ressler, K.J., Sullivan, S.L., and Buck, L.B. (1994). Information coding in the olfactory system: evidence for a stereotyped and highly organized epitope map in the olfactory bulb. *Cell* 79, 1245–1255.
- Roskams, A.J., Bethel, M.A., Hurt, K.J., and Ronnett, G.V. (1996). Sequential expression of Trks A, B, and C in the regenerating olfactory neuroepithelium. *J. Neurosci.* 16, 1294–1307.
- Royal, S.J., and Key, B. (1999). Development of P2 olfactory glomeruli in P2-internal ribosome entry site-tau-LacZ transgenic mice. *J. Neurosci.* 19, 9856–9864.
- Royet, J.P., Souchier, C., Jourdan, F., and Ploye, H. (1988). Morphometric study of the glomerular population in the mouse olfactory bulb: numerical density and size distribution along the rostrocaudal axis. *J. Comp. Neurol.* 270, 559–568.
- Ruiz, M.L., London, B., and Nadal-Ginard, B. (1996). Cloning and characterization of an olfactory cyclic nucleotide-gated channel expressed in mouse heart. *J. Mol. Cell. Cardiol.* 28, 1453–1461.
- Schaeren-Wiemers, N., and Gerfin-Moser, A. (1993). A single protocol to detect transcripts of various types and expression levels in neural tissue and cultured cells: in situ hybridization using digoxigenin-labelled cRNA probes. *Histochemistry* 100, 431–440.
- Schwenk, F., Baron, U., and Rajewsky, K. (1995). A cre-transgenic mouse strain for the ubiquitous deletion of loxP-flanked gene segments including deletion in germ cells. *Nucleic Acids Res.* 23, 5080–5081.
- Shepherd, G.M. (1994). Discrimination of molecular signals by the olfactory receptor neuron. *Neuron* 13, 771–790.
- Vassar, R., Chao, S.K., Sitcheran, R., Nunez, J.M., Vossahl, L.B., and Axel, R. (1994). Topographic organization of sensory projections to the olfactory bulb. *Cell* 79, 981–991.
- Zhao, H., Ivic, L., Otaki, J.M., Hashimoto, M., Mikoshiba, K., and Firestein, S. (1998). Functional expression of a mammalian odorant receptor. *Science* 279, 237–242.
- Zheng, C., Feinstein, P., Bozza, T., Rodriguez, I., and Mombaerts, P. (2000). Peripheral olfactory projections are differentially affected in mice deficient in a cyclic nucleotide-gated channel subunit. *Neuron* 26, 81–91.